

Research Article

Bioinformatics analysis of potential pathogenesis and risk genes of neuroinflammation-promoted brain injury in intracerebral hemorrhage

Ilgiz Gareev^{a,*}, Ozal Beylerli^a, Elmar Musaev^b, Chunlei Wang^c, Valentin Pavlov^a

^a Bashkir State Medical University, Ufa 450008, Russia

^b Sechenov First Moscow State Medical University, Moscow, Russian Federation

^c Department of Neurosurgery, The First Affiliated Hospital of Harbin Medical University, Harbin, Heilongjiang Province, Republic of China

ARTICLE INFO

Article history:

Received 30 May 2024

Received in revised form 15 July 2024

Accepted 23 July 2024

Available online 25 July 2024

Keywords:

Intracerebral hemorrhage

Bioinformatics analysis

miRNA–mRNA network

Neuroinflammation

Signaling pathways

Therapy

Prognosis

ABSTRACT

Objective: Spontaneous (non-traumatic) intracerebral hemorrhage (ICH) is one of the major causes of global death. The purpose of our bioinformatics analysis was to detect viable pathophysiological targets and small-molecule drug candidates and to identify the precise secondary mechanisms of brain injury in ICH.

Methods: The GSE24265 dataset, consisting of data from four perihematomal brain tissues and seven contralateral brain tissues, was downloaded from the Gene Expression Omnibus (GEO) database and screened for differentially expressed genes (DEGs) in ICH. Online analysis tool GEO2R and Drug Susceptibility Assessment Module within the ACBI Bioinformation tool was used for data differential expression analysis. TargetScan, miRDB, and RNA22 were used to investigate the miRNAs regulating the DEGs. The functional annotation of DEGs was performed using Gene Ontology (GO) resources, and the cell signaling pathway analysis of DEGs was performed using the Kyoto Encyclopedia of Genes and Genomes (KEGG). DAVID is used to perform GO function enrichment analysis and KEGG pathway analysis of candidate target genes. Enrichment analysis was performed for delving the molecular mechanism of DEGs, and protein–protein interaction (PPI) networks and microRNA (miRNA)–messenger RNA (mRNA) networks were used to reveal the hub nodes and the related interaction relationships. Hub genes and miRNA–mRNA interaction of PPI network were identified by STRING version 12.0 online software and Cytoscape. Next, the DEGs were analyzed using the L1000CDS2 database to identify small-molecule compounds with potential therapeutic effects.

Results: A total of 325 upregulated genes and 103 downregulated genes associated with ICH were identified. The biological functions of DEGs associated with ICH are mainly involved in the inflammatory response, chemokine activity, and immune response. The KEGG analysis identified several pathways significantly associated with ICH, including but not limited to cytokine–cytokine receptor interaction and MAPK signaling pathway. A PPI network consisting of 188 nodes and 563 edges was constructed using STRING, and 27 hub genes were identified with Cytoscape software. The miRNA–mRNA network with high connectivity contained key 27 mRNAs (from C–C motif chemokine ligand 5 (CCL5), C–C motif chemokine ligand 8 (CCL8), ..., to dishevelled-associated activator of morphogenesis 1 (DAAM1), and FRAT regulator of WNT signaling pathway 1 (FRAT1)) and 135 candidate miRNAs. These genes and miRNAs are closely related to secondary brain injury induced by ICH. In addition, a L1000CDS² analysis of six small-molecule compounds revealed their therapeutic potential.

Conclusions: Our study explores the pathogenesis of brain tissue injury promoted by neuroinflammation in ICH and extends the clinical utility of its key genes. At the same time, we constructed a miRNA–mRNA network which may play crucial roles in the pathogenesis of ICH. In addition, we obtained six small molecule compounds that will have anti-inflammatory effects on ICH, including Geldanamycin, Dasatinib, BMS-345541, Saracatinib, and Afatinib.

© 2024 International Hemorrhagic Stroke Association. Publishing services by Elsevier B.V. on behalf of KeAi Communications Co. Ltd. This is an open access article under the CC BY-NC-ND license (<http://creativecommons.org/licenses/by-nc-nd/4.0/>).

* Corresponding author at: Bashkir State Medical University, Ufa 450008, Russia

E-mail address: ilgiz_gareev@mail.ru (I. Gareev).

1. Introduction

Spontaneous (non-traumatic) intracerebral hemorrhage (ICH) is a polyetiological nosologically form characterized primarily by parenchymal hemorrhage. The prognosis for ICH is generally unfavorable where the overall mortality rate reaches 60–70 %. According to consolidated world studies, 35–50 % of patients die in the first 30 days after ICH, half of them in the first 2 days^{1,2}.

It is now known that ICH includes not only the primary brain lesions caused by the hematoma due to direct damage to the tissues around the hematoma, but also includes intoxications caused by lysis of red blood cells, oxidative stress, toxic effects of excitatory amino acids and neuroinflammation of the tissue surrounding the hematoma, which causes secondary damage.³ Secondary damage to the brain parenchyma caused by ICH contributes to neurological disorders, which manifest themselves at the cellular level in the form of neuronal apoptosis and glial cells activation and proliferation.⁴ Like the “ischemic penumbra” in cerebral infarction, the tissue around the hematoma, due to the lack of a clear definition, is conventionally called the “microenvironment” of the hematoma.⁴ Directly investigating the molecular mechanisms underlying changes in the hematoma microenvironment after ICH may provide a better understanding of the pathological mechanisms underlying ICH, thereby aiding in the development of diagnostic and therapeutic tools. For instance, several studies have attempted to correlate changes in the expression levels of microRNAs (miRNAs) and corresponding target genes in ICH, both *in vitro* and *in vivo*, in order to elucidate the mechanisms of ICH pathogenesis and subsequent processes including neuroinflammation.^{5–7}

Since many of the regulatory processes (including miRNA-messenger RNA (mRNA) regulatory network) necessary to maintain the functions of brain cells after strokes have already been identified, it is possible to conduct a targeted and systematic study of the signaling pathways involved in these pathways using bioinformatics research in patients with an established diagnosis of ICH. Bioinformatics analysis can use next-generation sequencing (NGS) technology to analyze the genomic, transcriptomic, and proteomic information of organisms, and reveal the mechanism of disease occurrence and development at various molecular levels, providing direction for clinical research.^{8,9} By analyzing the biological functions associated with ICH, it is possible to lay the foundation for clinical diagnosis and treatment of this dangerous disease. In this study, the original dataset GSE24265 was selected to screen for differentially expressed genes (DEGs) between the ICH samples and the normal brain samples as control group. To evaluate the potential molecular mechanism of ICH regulation, DEGs were further analyzed by Gene Ontology (GO) and Kyoto Encyclopedia of Genes and Genomes (KEGG) pathway analysis based on the Database for Annotation, Visualization and Integrated Discovery (DAVID). In addition, the DEGs were analyzed using the L1000CDS² database to identify small-molecule compounds with potential therapeutic effects on ICH. Finally, we provide a bioinformatic analysis of DEGs and predicted miRNAs for ICH patients.

2. Matherail amd methods

2.1. Data collection

The gene expression profiles were obtained from Gene Expression Omnibus (GEO) database (<http://www.ncbi.nlm.nih.gov/geo/>, accessed 20/05/2024) which is public availability. We downloaded the GSE24265 annotated by GPL570 [HG-U133_Plus_2] Affymetrix Human Genome U133 Plus 2.0 Array where dataset contains brain tissues from 4 patients with ICH. Perihematomal areas were used for the disease groups (n = 4), while the contralateral grey (n = 4)

and white matter (n = 3) were used as controls.^{10,11} We used GEO2R and GEO Date Analysis Module within the ACBI Bioinformatics tool (<https://www.aclbi.com/static/index.html#/geo>) to analyze DEGs between the disease groups and controls from GSE24265 database.¹² Adjusted P value < 0.05 and (|log2 FC (fold change)|) > 2 were identified as the starting point of DEGs. Fig. 1 demonstrates the workflow of the study.

2.2. GO and KEGG analyses

To enable better recognition of the biological functions of DEGs, we used online tools to perform GO enrichment and KEGG analyses. Functional annotation analysis of the DEGs was performed using DAVID, and the GO analysis and KEGG-assisted cell signaling pathway analysis of the DEGs was carried out using GEO Date Analysis Module within the ACBI Bioinformatics tool (<https://www.aclbi.com/static/index.html#/geo>).¹² P-values of < 0.05 were considered to be statistically significant.

2.3. Identification of protein–protein interaction (PPI) networks of DEGs

PPI networks were built in the STRING version 12.0 online software (<https://string-db.org/> (accessed on 23 May 2024)). The minimum required interaction score was ≥ 0.400 . The molecular complex detection plug-in was served as a tool to select gene modules with MCODE score ≥ 3.50 . A new method, maximal clique centrality (MCC), was recently proposed to be better than the other methods; therefore, we selected hub genes with the cytoHubba plugin using MCC methods.¹³ Furthermore, the KEGG analysis of modules was done by Metascape.

2.4. Identifying miRNA-mRNA interaction

Three online databases, including TargetScan (https://www.targetscan.org/vert_80/), miRDB (<https://mirdb.org/custom.html>), and RNA22 (<https://cm.jefferson.edu/rna22/>), were used to investigate the miRNAs regulating the DEGs. These databases contain the experimentally validated associations between miRNAs and mRNAs. MiRNAs with the highest score were included in the interaction network, context++ score percentile > 95 (The context++ score percentile rank is the percentage of sites for this miRNA with a less favorable context++ score) by TargetScan and Target Score > 85 by miRDB. In additional, high confidence is assigned when the Weighted context++ score determined by TargetScan is -0.4 or lower. Such estimates predict that miRNA suppresses a particular mRNA target by at least 25 % relative to normal levels. Moderate confidence is assigned when the Weighted context++ score is between -0.2 and -0.4 . Such estimates predict that miRNAs suppress a specific mRNA target by 13–25 % of their normal levels.^{14,15} Eventually, the final miRNA-mRNA interactions were visualized using Cytoscape software (version 3.10.1).

2.5. Identification of candidate small molecule drugs for ICH

First, the DEGs were classified into up-regulated and down-regulated groups. Then, these genes from two groups were uploaded into L1000CDS² database (<https://maayanlab.cloud/L1000CDS2/#/index>). This L1000CDS2 is the library of chemically perturbed different cell lines exposed to small molecular agents. This online tool helps to search L1000 small molecule signatures that match user input signatures (i.e., upregulated and downregulated genes). To determine the statistical significance of the identified drugs (p-value) and similarity score, the Kolmogorov–Smirnov statistic and random permutation tests were used. A p-value < 0.05 with the reversal effect on the DEGs signatures was utilized to

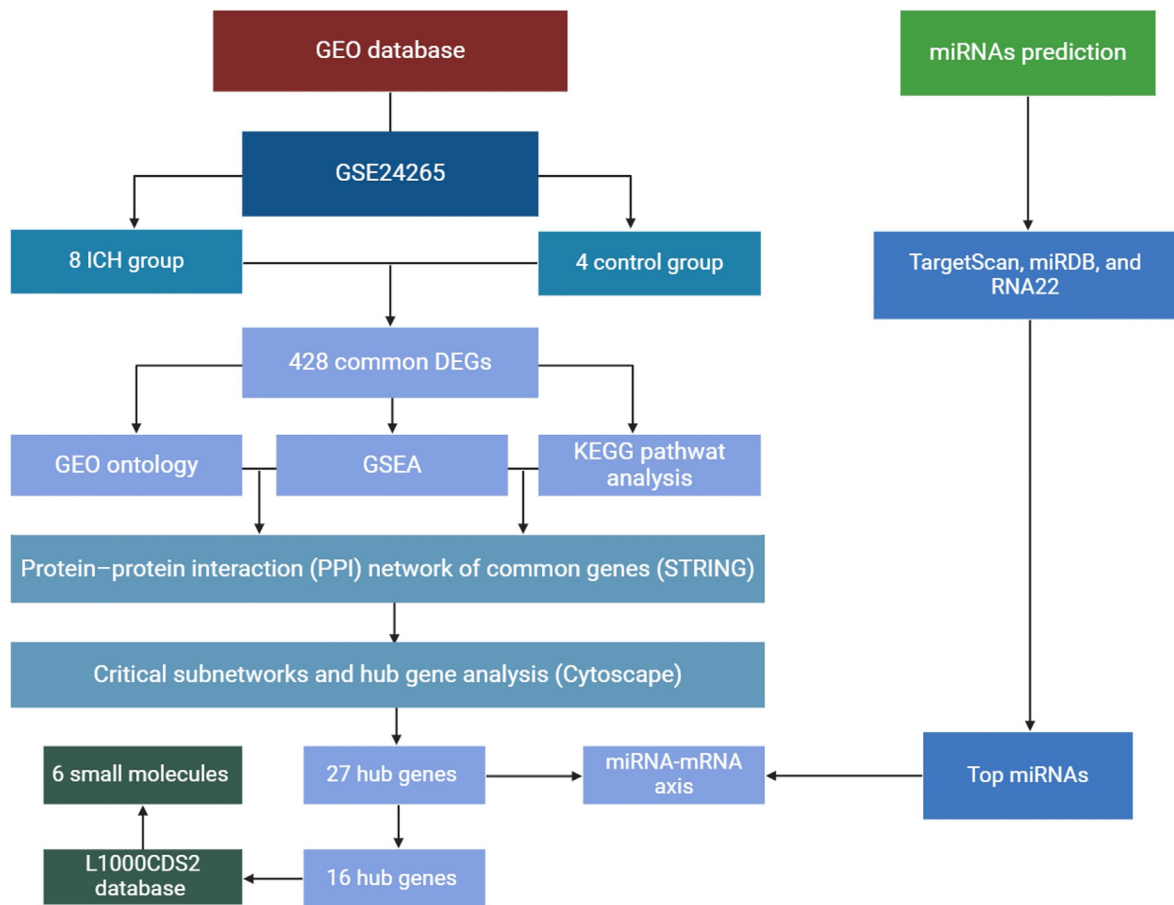


Fig. 1. The workflow of the study.

select potential anti-inflammatory and neuroprotective drug candidates in ICH. The indications and mechanism of action information for the drugs was collected from the National Center for Biotechnology Information (NCBI)-PubChem database.

3. Results

3.1. Identification of DEGs in ICH

The gene expression profile of the GSE24265 dataset contained data obtained from 4 perihematoma tissues and 7 contralateral tissues. Using a P-value of < 0.05 and a $|\log FC|$ of > 2 as the cut-off, a total of 428 DEGs, including 325 upregulated and 103 downregulated genes, were obtained on comparison of the expression profiles between the disease groups and control groups (Table 1). Heat maps and volcano plots for the distribution of DEGs were generated using R software (Fig. 2 A-B).

3.2. Functional annotation analysis of DEGs using GO

GO enrichment analysis for upregulated and downregulated genes revealed Top 20 related GO functions ($p < 0.05$) involving a large number of pathways that might be related to neutrophil degranulation, neutrophil activation involved in immune response, leukocyte cell – cell adhesion, and cell – substrate junction (Fig. 3 A-B).

3.3. KEGG pathway analysis of DEGs

The results of the cell signaling pathway enrichment analysis of the DEGs identified a total of Top 30 meaningful pathways which were analyzed. The results of KEGG analysis showed that upregulated genes are activated in biological processes including cytokine – cytokine receptor interaction, viral protein interaction with cytokine and cytokine receptor, tumor necrosis factor (TNF) signaling pathway, rheumatoid arthritis, phagosome, lipid and atherosclerosis. Downregulated genes were mainly involved in cellular signaling pathways which clearly associated Wnt signaling pathway. The specific enriched pathways obtained from the analysis of the DEGs are summarized in and [Fig. 4 A-B](#).

The latest, the cytokine – cytokine receptor interaction is significantly correlated with pathogenesis of ICH, and includes the 23 upregulated genes as C-C motif chemokine ligand 5 (CCL5), C-C motif chemokine ligand 8 (CCL8), C-C motif chemokine ligand 2 (CCL2), C-C motif chemokine ligand 20 (CCL20), C-X-C motif chemokine ligand 1 (CXCL1), C-X-C motif chemokine ligand 5 (CXCL5), C-X-C motif chemokine ligand 8 (CXCL8), pro-platelet basic protein (PPBP), C-X-C motif chemokine ligand 12 (CXCL12), C-X-C motif chemokine ligand 16 (CXCL16), C-X-C motif chemokine receptor 4 (CXCR4), interleukin 7 receptor (IL7R), interleukin 13 receptor subunit alpha 1 (IL13RA1), interleukin 6 (IL6), LIF interleukin 6 family cytokine (LIF), interleukin 1 beta (IL1B), interferon gamma receptor 1 (IFNGR1), interleukin 1 receptor type 1 (IL1R1), interleukin 1 receptor type 2 (IL1R2), interleukin 18 receptor accessory protein (IL18RAP), TNF receptor superfamily member 1B

Table 1
Screening differentially expressed genes (DEGs) in intracerebral hemorrhage (ICH).

DEGs	Gene terms
Upregulated	BZW1, TES, RASSF3, GPAT3, VGLL3, SPHK1, BLVRB, ANXA5, CD63, HLA-A, AKR1C2, METRNL, CHIC2, KDM7A, SLC2A14, ANXA2, UPP1, TNFRSF12A, G0S2, LGALS1, ARHGAP18, ITGA5, B3GNT5, HLA-B, PMAIP1, MAPRE1, PROCR, DNAJA4, RPL8, SLC2A3, VASP, BCAT1, HLA-C, ORMDL2, FTL, TNFAIP3, GBE1, ARF4, VCAM1, SH3BGR13, VMP1, CXCL1, ERO1A, COL1A2, DPH3, ITGAX, MYH9, RPLP0, ISG20,HLA-F, DDIT3, PLAUI, HMOX1, C15ORF48, RPS2, PLAUR, DUSP5, LAPTM5, CCN2, IFI30, CYSTM1, SYAP1, LCP1, ALOX5AP, CTS1, CXCL16, FGR, SERPINE1, MYCT1, ESM1, IL18RAP, GPRC5A, KLHL6, PTGS1, OAZ1, NOD2, STAT3, SAT1, RUBCNL, LYZ, RPS5, OCIA2, HSPB1, CCRL2, ZFAND2A, VNN2, FCER1G, ATP13A3, COTL1, TFPI2, CXCL8, MYO1F, C11ORF96, CCL20, TUBB6, UCK2, CYTIP, CXCL3, VKORC1, SH3D21, MPP1, SMIM3, RACK1, GRPEL1, PROK2, BCL2A1, C5AR1, MGAM, CPVL, VAMP8, KLF4, IL1R1, PPP1R15A, ETS1, THBS1, TREM1, COL6A3, GZMB, GPCPD1, OST4, CD93, IRAK3, RILPL2, LSMEM1, CXCR4, MYADM, HPGDS, RGS16, CDH5, THBD, RPGR, CD68, STK40, EMG1, CDCP1, HCLS1, FN1, SLC11A1,MCEMP1, ATF4, TYROBP, GNG5, PFN1, TGFB1, FERMT3, PNP, HBG1, OLR1, BHLHE40, S100A11, TKT11, PLEK, COL4A1, NCF2, PPBP, STC1, CSTA, CXCL2, SRGN, RRAS2, PLA2G7, B2M, SEC24A, PDLIM1, HSPA6, SDC2, TCIRG1, INPP5F, CAV1, HCAR3, ADM, IFNGR1, ANXA1, FLNA, GPX1, IL1R2, TM4SF1, DSP, RPL35, CCL8, RPL22L1, NABP1, RGS1, GCH1, TGFB1I1, HAS1, HLA-DRB1, SLA, HBD, SYTL3, CD69, HBB, CLIC4, IL6, TP53I3, SQOR, MMP3, SDCBP2, COL4A2, HLA-DRA, RFLNB, BCL10, PTX3, GZMA, NFKBIE, ZPR1, MAP2K3, PLIN2, C12ORF75, CST7, PSMD8, ICAM1, PLP2, TIMP1, CCL3, SERPINH1, CA2, SLC16A3, CAV2, SAMSN1, ARG2, MARCO, IL13RA1, RGS2, TNFRSF1B, NBPFF20, CD59, HLA-DQA1, PPP1R18, CAPG, MANF, ALDH1A2, CD55, OSTC, CTSC, LIF, TLR2, HBA1, CXCL12, CCL4, LAMC1, ADGRL4, TFPI, CCL5, PTPRC, CLIC1, OLFML3, LMCD1, SELE, CXCL5, VEGFA, EIF6, SLC7A7, MT2A, CLEC5A, CLEC2B, SLC25A37, GNA13, TMEM71, AKAP12, HLA-DPA1, EMP1, CYBSR2, SERPINB2, IER3, SOD2, CTSS, FOSL1, ZNF367, MAD2L2, GPR183, ATF3, RHOF, NLRP3, SPP1, IL7R, REL, TNFAIP8, HLA-DRB5, EMP3, GNA15, S100P, CD163, INHBA, SLC16A6, MS4A4A, GMFG, ACSL5, GZMH, CCN1, EVI2B, CRYAB, LDHA, HPSE, ECSCR, NAMPT, GPNMB, DNAJB1, BIRC3, S100A4, CCL2, HLA-DQB1, CTHRC1, MAFF, FGFBP2, SOX7, MXD1, BACE2, ACSL1, DDIT4, CKS2, PCOLCE2, HBM, FCN1, GPR160, NFKBIZ, ANGPT2, PELI1, TPM4, CITED1, IL1B, MCUB, ETS2, GBP2, and TM4SF18
Downregulated	ZNF540, NIM1K, PWWP3B, DAAM1, FIGN, BHLHE22, ADGRB3, CRB1, NEURL1B, PCYOX1L, PRDM16, FAM133A, MAST3, PPM1K, MAN1C1, BMPR1B, ZNF436, NUA1K, NDP, PDIK1L, BICRAL, ZNF329, SLITRK5, SHROOM2, RELN, TLCD4, RHOBTB1, MTCL1, SOWAHA, ZNF703, ARNT2, EMX2, CALN1, ZNF623, CRLF1, IP6K1, SOX9, NR3C2, PRC1, TOB1, SLIT2, SLITRK1, KIAA0232, CNTN3, GRIA2, SLC39A11, KCTD4, TMEM178A, KIRREL3, RYR2, PTCHD1, SYT17, SATB1, FAM217B, PAX6, ZNF136, PCDH10, CELSR2, LDB2, ZNRF3, INSM1, PIRT, CHRDL1, NINL, NEGR1, YPEL4, KBTBD7, DCBLD1, ARX, CBX7, FRAT1, SORCS2, FXYD6, NTN4, FZD3, NANP, TMEM132B, GLCE, TMEM170B, LANCL3, BRINP3, FAM189A2, PRRT2, CRISPLD1, LHX2, MPPED1, PLCXD3, EID2B, SLC8A2, PRICKLE2, PNMA8B, PSD3, FOXG1, CACNA2D3, PRAG1, ZNF304, SGIP1, HYLS1, FRMPD2, LRP2BP, NXPH1, CACNG3, and SCAI

(TNFRSF1B), TNF receptor superfamily member 12A (TNFRSF12A), and inhibin subunit beta A (INHBA) (Fig. 5).

In parallel, Wnt signaling pathway is significantly correlated with pathogenesis of ICH and includes the 5 downregulated genes as Frizzled-3 (FZD3), zinc and ring finger 3 (ZNRF3), prickle planar cell polarity protein 2 (PRICKLE2), dishevelled-associated activator of morphogenesis 1 (DAAM1), and FRAT regulator of WNT signaling pathway 1 (FRAT1) (Fig. 6). We next constructed a miRNA-mRNA interaction network to better elucidate the brain tissue damage in ICH.

3.4. PPI network and analysis of the modules

We uploaded 428 DEGs to the string online database to obtain the PPI network. The resulting PPI network contained a total of 188 nodes and 563 edges. Fig. 7 presents the visualization of the network generated using STRING version 12.0 online software. The KEGG pathway analysis showed that the module genes are majorly contacted with the cytokine – cytokine receptor interaction and MAPK signaling pathway (see above). The top 27 hub genes selected by MCC were CCL5, CCL8, CCL2, CCL20, CXCL1, CXCL5, CXCL8, PPBP, CXCL12, CXCL16, CXCR4, IL7R, IL13RA1, IL6, LIF, IL1B, IFNGR1, IL1R1, IL1R2, IL18RAP, TNFRSF12A, INHBA, FZD3, ZNRF3, PRICKLE2, DAAM1, and FRAT1.

3.5. Validation of miRNA-mRNA network

Prediction analysis using TargetScan, miRDB, and RNA22 bioinformatic tools identified the top 5 selected miRNAs targeting each 22 upregulated and 5 downregulated genes involved in ICH pathogenesis across the cytokine – cytokine receptor interaction and MAPK signaling pathway and these data appear in Table 2 and Table 3.

To foster intuitive understanding of the regulatory mechanism of the key neuroinflammatory genes, the miRNA-mRNA networks of the key genes were shown in Fig. 8. Among these, hsa-miR-19b-3p, hsa-miR-19a-3p, hsa-miR-548at-5p, hsa-miR-5692a, hsa-miR-3688-3p, hsa-miR-379-5p, hsa-miR-4536-5p, hsa-miR-29b-3p, and hsa-miR-29a-3p have a higher number of connecting nodes; therefore, they might be more significant in ICH. These data enable us to understand how predicted miRNAs are related to ICH progress.

3.6. L1000CDS² analysis

To assess the potential drugs to therapeutically target identified DEGs, we have utilized the LINCS L1000 connectivity map data and characteristic direction signature search engine L1000CDS². The list of DEG was entered into a web tool to search for substances that can reverse the expression changes in identified DEGs. 35 drugs or small molecules were identified, showing potential with an overlap score of > 0.2 to reverse expression profiles on upregulated and/or downregulated gene expressions in cell lines (Fig. 9). We selected 13 out of 35 existing drugs or small molecules with an overlap score of > 0.25 (Table 4).

A considerable portion (6 out of 13) of the drugs was anti-inflammatory and potential neuroprotective effect agents (information is also based on literature search), which were suggested for the treatment and management of the ICH (Fig. 10 and Table 5). They possess the potential to reverse the expression of the top 16 out of 27 DEGs which are involved in the inflammatory process as shown in our analysis.

4. Discussion

Neuroinflammation is a pivotal response following ICH, initiated by the presence of blood byproducts in the subarachnoid space and/or brain parenchyma. This inflammatory process is marked by the activation of resident immune cells, such as microglia and astrocytes, along with the infiltration of peripheral immune cells. These activated immune cells release a variety of pro-inflammatory cytokines, chemokines, and reactive oxygen species (ROS), which contribute to significant pathophysiological changes. The resultant inflammatory mediators are instrumental in disrupting the blood-brain barrier (BBB), causing neuronal damage, and leading to cerebral edema. This cascade of events

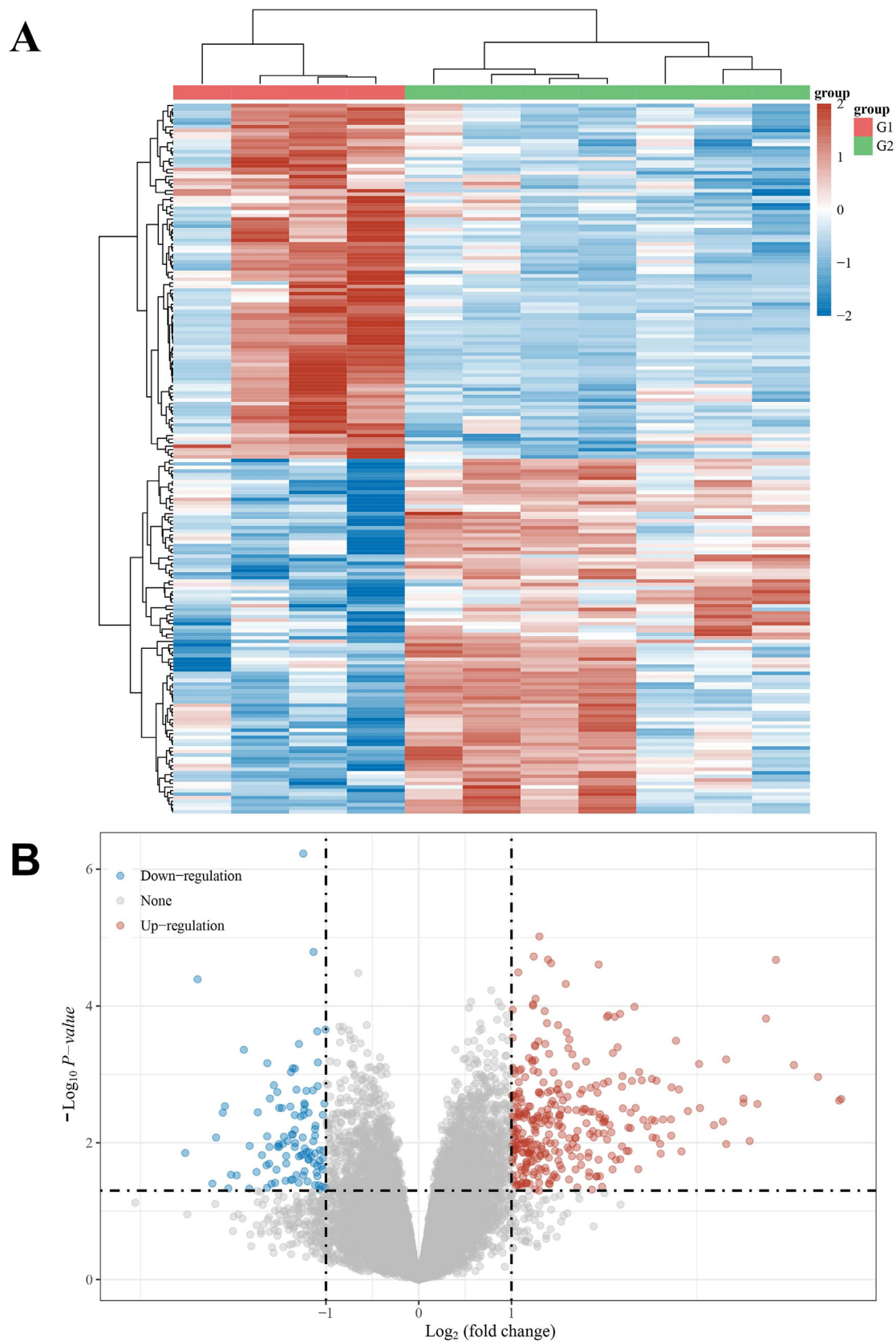


Fig. 2. Differentially expressed genes (DEGs) from GSE24265. (A) The expression data is represented as a data matrix wherein each row represents a gene, and each column represents a sample. The green coded bar above the heat map represents the normal sample set and the red coded bar represents the perihematomal sample. The expression level is described in terms of the color ratio of the upper left corner. (B) Differential expression volcano map among 428 DEGs. (For interpretation of the references to color in this figure legend, the reader is referred to the web version of this article.)

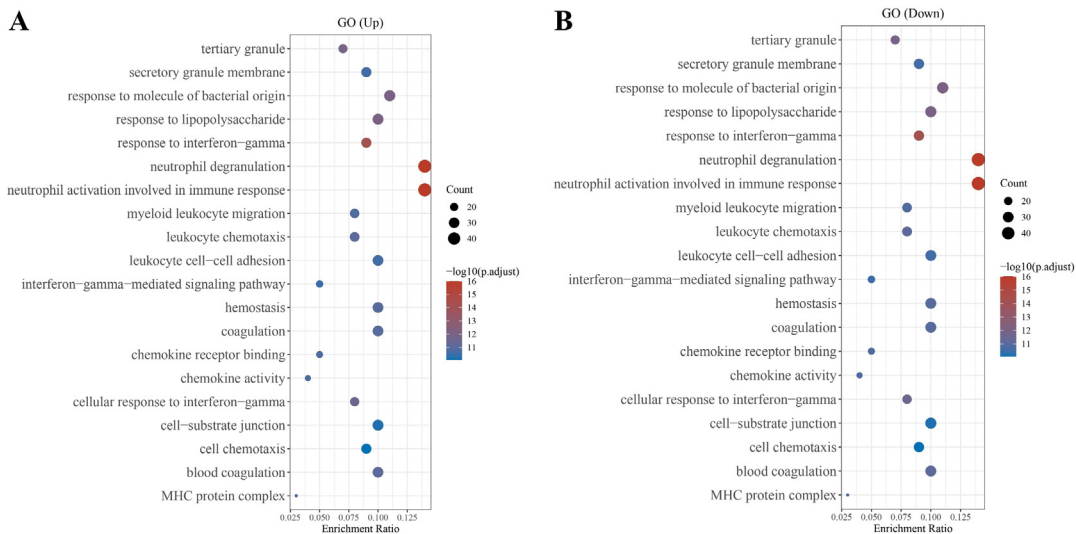


Fig. 3. Gene Ontology (GO) enrichment analysis result of (A) upregulated and (B) downregulated genes with $|\log FC| \geq 2$.

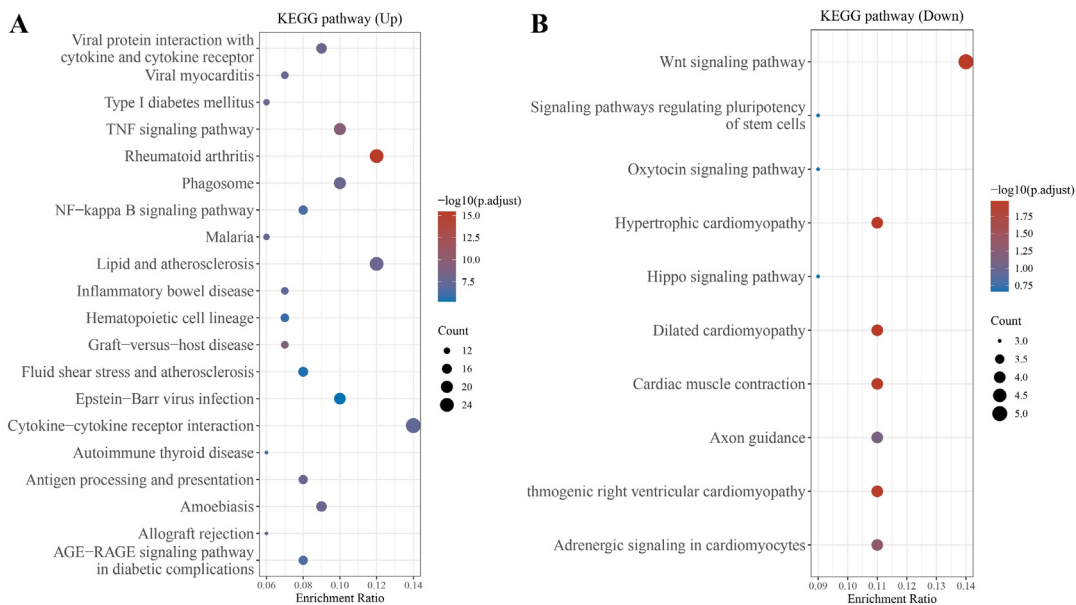


Fig. 4. Kyoto Encyclopedia of Genes and Genomes (KEGG) pathway analysis of the (A) upregulated and (B) downregulated genes in intracerebral hemorrhage (ICH).

promotes neuronal apoptosis and impairs neuroplasticity, thereby exacerbating the neurological deficits associated with ICH. Despite these detrimental effects, neuroinflammation also has potential beneficial roles. It aids in clearing cellular debris and promoting tissue repair, highlighting its dualistic nature. In the acute phase of ICH, the rapid activation of microglia and astrocytes leads to the production of inflammatory mediators such as TNF- α , interleukins (e.g., IL-1 β and IL-6), and interferons.^{3,4} These substances exacerbate the inflammatory response, leading to further neuronal injury and the amplification of the neuroinflammatory cycle. Simultaneously, the disruption of the BBB allows peripheral immune cells, including neutrophils, monocytes, and lymphocytes, to infiltrate the brain tissue, further contributing to the inflammatory milieu. The chronic phase of neuroinflammation in ICH is characterized by sustained activation of glial cells and continued infiltration of peripheral immune cells. This prolonged inflammatory state can lead to ongoing neuronal damage, synaptic dysfunction, and inhibition of neurogenesis, severely impacting the brain's ability to recover and adapt post-

injury. However, during this phase, the resolution of inflammation and initiation of repair mechanisms also occur. Microglia can shift towards an anti-inflammatory phenotype, secreting factors that promote tissue repair, angiogenesis, and neuronal survival. Given the dual role of neuroinflammation in ICH, therapeutic strategies need to be carefully balanced to mitigate the harmful effects while enhancing the beneficial aspects. Understanding its mechanisms, phases, and cellular players is essential for developing effective therapies. By modulating the neuroinflammatory response, it is possible to reduce secondary injury, promote recovery, and ultimately improve outcomes for patients with ICH. The complex interplay between detrimental and beneficial effects of neuroinflammation underscores the need for ongoing research to identify optimal therapeutic strategies that address the multifaceted nature of this response. The results of our study provide new insight into the pathophysiology of neuroinflammation, highlighting the potential of targeting specific cytokines and chemokines with a range of small molecules as therapeutic strategies.

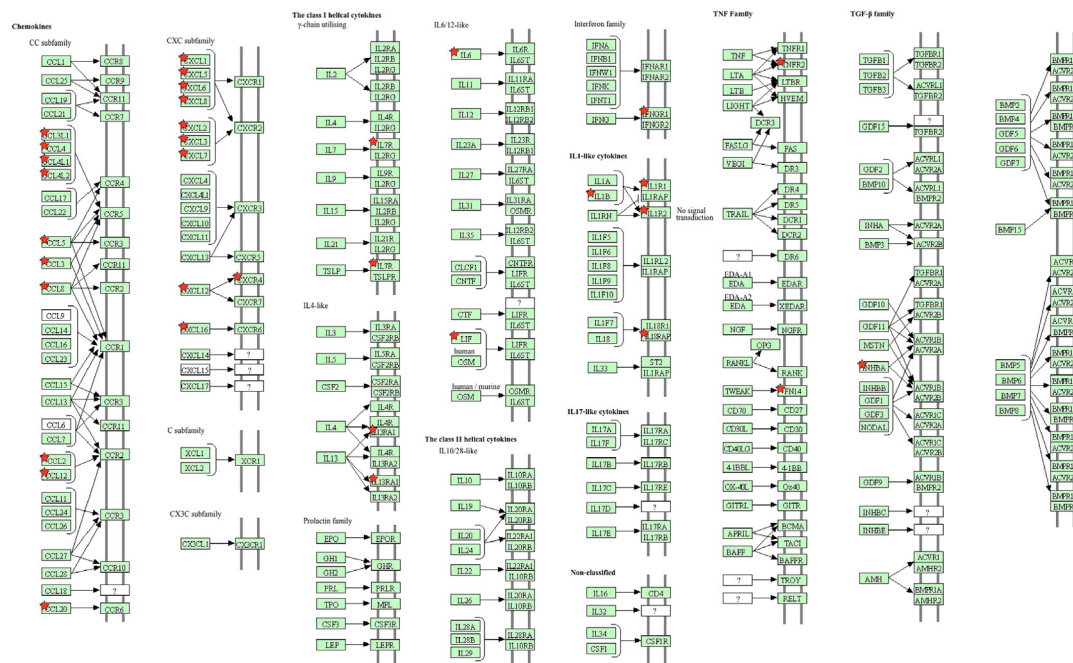


Fig. 5. The cytokine – cytokine receptor interaction is the significant pathway of the source genes (red background) of differentially expressed genes (DEGs) in intracerebral hemorrhage (ICH). (For interpretation of the references to color in this figure legend, the reader is referred to the web version of this article.)

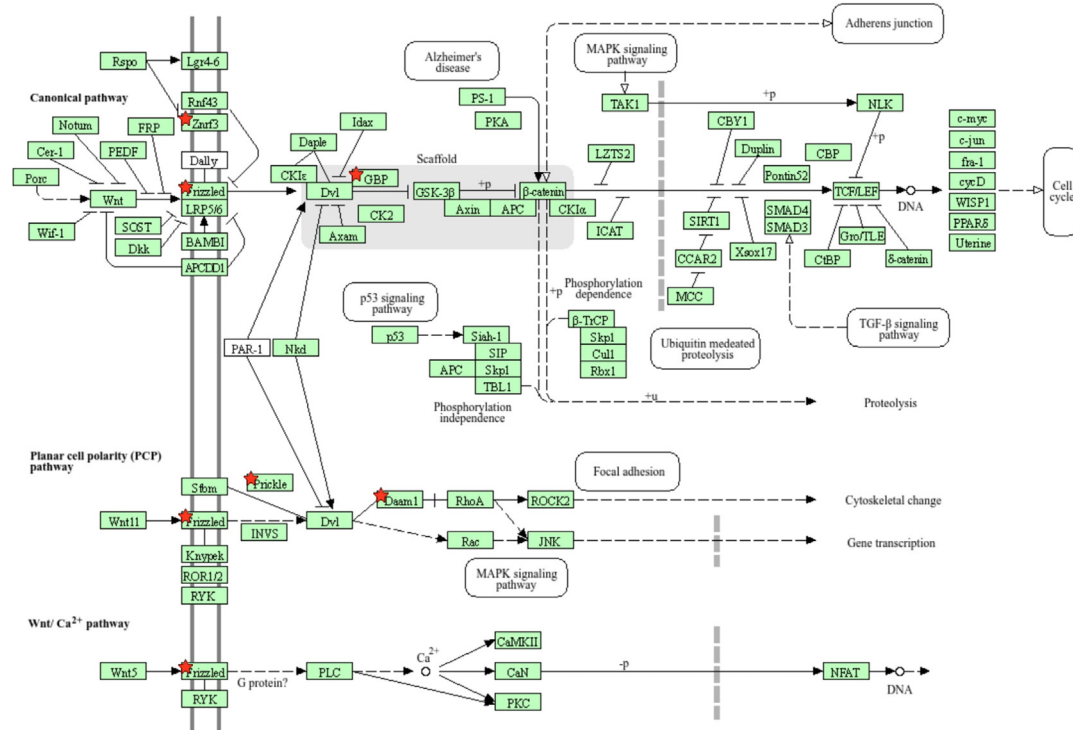


Fig. 6. MAPK signaling pathway is the significant pathway of the source genes (red background) of differentially expressed genes (DEGs) in intracerebral hemorrhage (ICH). (For interpretation of the references to color in this figure legend, the reader is referred to the web version of this article.)

The present study uses the GEO database to obtain gene expression profiles from patients with ICH and screens for DEGs. We perform functional enrichment analyses on the obtained DEGs to understand their biological functions. Meanwhile, we report meaningful enrichment, by KEGG analysis, of pathways involved in triggering the regulatory pathway associated with neuroinflammation as secondary brain injury induced by ICH. At the same time, an online prediction database, TargetScan, miRDB, and RNA22 was

used to obtain interactions with high confidence class between key mRNAs and potential miRNAs. The current study examined various molecular targets and signaling pathways involved in neuroinflammation, such as the cytokine – cytokine receptor interaction and Wnt signaling pathway. After importing the interactions into Cytoscape, a miRNA-mRNA network consisting of 27 mRNAs and 135 miRNAs was obtained. In addition, several potential small-molecule compounds, related to ICH, were identified by

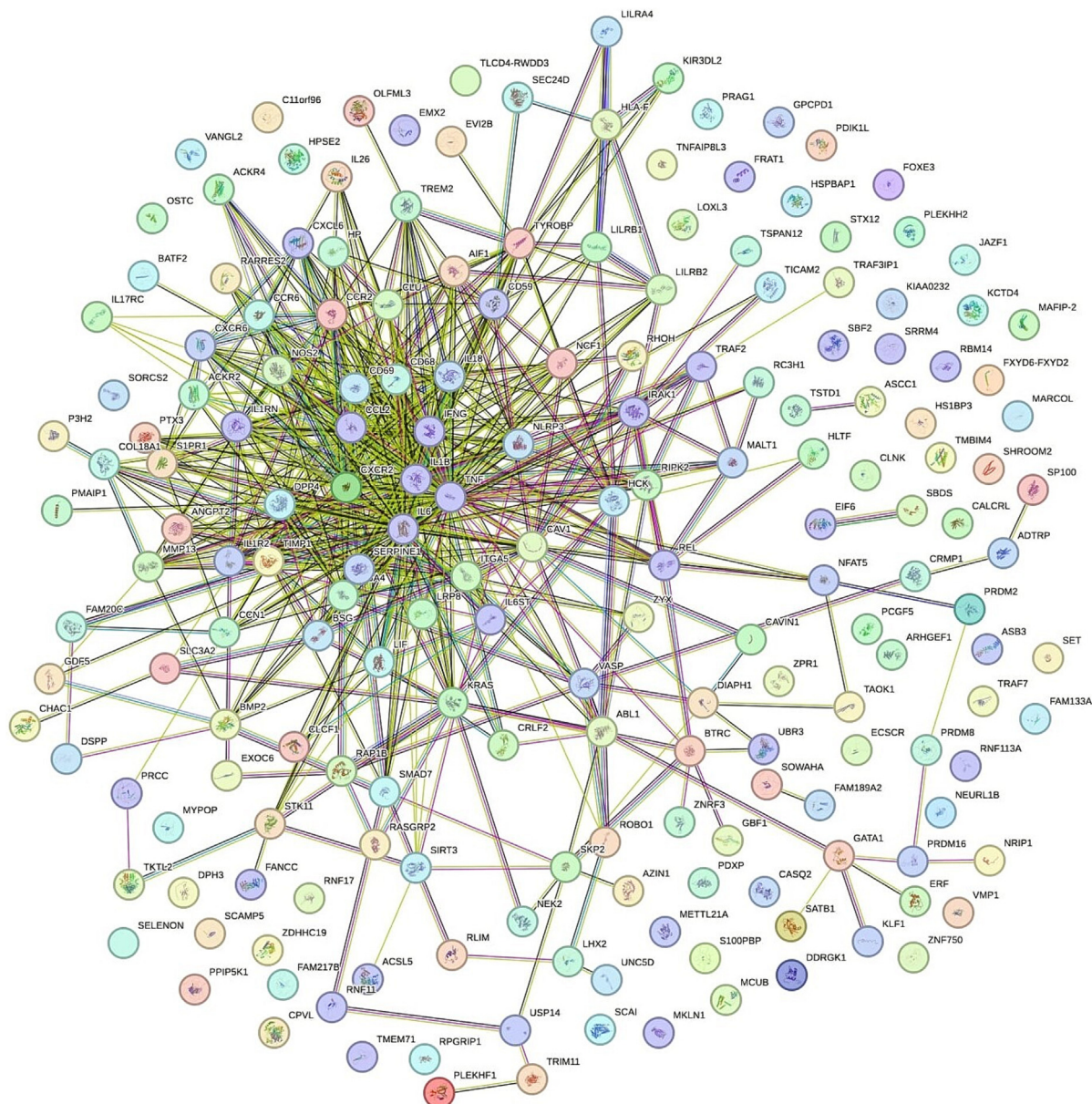


Fig. 7. Protein–protein interaction (PPI) network of differentially expressed genes (DEGs). The PPI network was created from 428 DEGs obtained from the GSE24265 database using STRING version 12.0 online software.

L1000CDS² analysis. These may become effective drugs for treating ICH in future.

Primary brain injury from ICH typically occurs within the first few hours of ictus and is due to hematoma formation, leading to mechanical damage of the adjacent tissues from dissection and compression. Although recent minimally invasive surgical approaches to hematoma removal while limiting surgical morbidity are underway with promising results, this does not address the secondary brain injury following ICH.³⁵ It has become increasingly clear that the cellular and molecular components of inflammation are involved in post-ICH secondary brain injury and are key components to the overall outcome of ICH.³⁵ The need for new therapeutic approaches for ICH has prompted a search for the molecular and cellular mechanisms that underlie early and delayed brain damage after ICH. From the GSE24265 dataset, after comparing the gene expression data obtained from ICH tissue with that obtained from the contralateral brain tissues, we obtained 325 upregulated and 103 downregulated DEGs. GO and KEGG analysis indicated that the main functional annotation results were consis-

tent with those obtained by previous reports, i.e., a significant increase in inflammatory response promotes ICH-induced brain injury, which may be one of the main factors contributing to the poor prognosis in patients with ICH.^{11,12} Previous reports have indicated that the cellular signaling pathways identified in this study using a KEGG analysis were closely related to cerebral hemorrhage; those activated within a few hours after cerebral hemorrhage, including the cytokine – cytokine receptor interaction, which participates in the secondary inflammatory reactions and formation of cerebral edema around the hematoma and the Wnt signaling pathway, which modulates of inflammatory cytokine production, and participation in innate defense mechanisms as well as in the bridging of innate and adaptive immunity.^{36–39} Both the cytokine – cytokine receptor interaction and Wnt signaling pathway play a critical regulatory role in the secondary brain. Twenty-seven regulated genes including CCL5, CCL8, CCL2, CCL20, CXCL1, CXCL5, CXCL8, PPBP, CXCL12, CXCL16, CXCR4, IL7R, IL13RA1, IL6, LIF, IL1B, IFNGR1, IL1R1, IL1R2, IL18RAP, TNFRSF12A, INHBA, FZD3, ZNRF3, PRICKLE2, DAAM1, and FRAT1

Table 2

MicroRNAs (miRNAs) selection and Co- differentially expressed genes (Co-DEGs) by TargetScan.

Genes	Predicted miRNAs	Context++ score percentile	Weighted context++ score
CCL5	hsa-miR-4650-3p	99	−0.50
	hsa-miR-4536-5p	99	−0.59
	hsa-miR-6742-3p	99	−0.44
	hsa-miR-6780b-5p	99	−0.53
	hsa-miR-4259	99	−0.58
CCL8	hsa-miR-181d-5p	98	−0.39
	hsa-miR-181c-5p	98	−0.37
	hsa-miR-4262	98	−0.30
	hsa-miR-181a-5p	98	−0.39
	hsa-miR-181b-5p	98	−0.39
CCL2	hsa-miR-345-5p	99	−0.63
	hsa-miR-3188	99	−0.57
	hsa-miR-301a-5p	99	−0.58
	hsa-miR-301b-5p	99	−0.60
	hsa-miR-493-5p	99	−0.54
CCL20	hsa-miR-590-5p	99	−0.69
	hsa-miR-21-5p	99	−0.75
CXCL1	hsa-miR-203a-3p	96	−0.21
	hsa-miR-655-3p	99	−0.49
PPBP	hsa-miR-374c-5p	99	−0.48
	hsa-miR-3192-5p	99	−0.41
CXCL12	hsa-miR-1343-3p	99	−0.66
	hsa-miR-6783-3p	99	−0.66
	hsa-miR-3605-5p	99	−0.64
	hsa-miR-670-3p	99	−0.45
	hsa-miR-5693	99	−0.66
CXCL16	hsa-miR-6797-3p	99	−0.55
	hsa-miR-3688-3p	99	−0.68
	hsa-miR-6827-3p	98	−0.58
	hsa-miR-340-3p	98	−0.56
	hsa-miR-4433a-3p	99	−0.38
IL7R	hsa-miR-7106-5p	99	−0.39
	hsa-miR-4536-5p	98	−0.45
	hsa-miR-6501-5p	99	−0.63
	hsa-miR-4701-5p	99	−0.65
	hsa-miR-588	99	−0.68
IL13RA1	hsa-miR-4266	99	−0.70
	hsa-miR-4779	99	−0.76
	hsa-miR-199a-3p	97	−0.34
	hsa-miR-3129-5p	97	−0.28
	hsa-miR-199b-3p	97	−0.34
IL6	hsa-miR-760	99	−0.57
	hsa-miR-149-5p	99	−0.55
LIF	hsa-miR-7-5p	98	−0.35
IL1B	hsa-miR-4727-5p	99	−0.52
	hsa-miR-6738-3p	98	−0.42
IFNGR1	hsa-miR-1291	99	−0.53
	hsa-miR-6775-3p	98	−0.52
	hsa-miR-3937	99	−0.63
	hsa-miR-7154-5p	99	−0.37
	hsa-miR-224-5p	99	−0.40
IL1R1	hsa-miR-1243	99	−0.49
	hsa-miR-3914	97	−0.31
	hsa-miR-675-3p	97	−0.32
	hsa-miR-19b-3p	96	−0.34
	hsa-miR-19a-3p	96	−0.34
IL1R2	hsa-miR-6508-5p	98	−0.28
	hsa-miR-8067	98	−0.29
	hsa-miR-5195-5p	99	−0.61
	hsa-miR-183-3p	99	−0.40
	hsa-miR-379-5p	99	−0.39
IL18RAP	hsa-miR-891a-3p	99	−0.39
	hsa-miR-4540	99	−0.45
	hsa-miR-8087	99	−0.34
	hsa-miR-4515	98	−0.43
	hsa-miR-1915-3p	99	−0.47
TNFRSF12A	hsa-miR-6782-5p	99	−0.56
	hsa-miR-3529-5p	99	−0.62
	hsa-miR-379-5p	99	−0.60
	hsa-miR-19b-3p	99	−0.47
	hsa-miR-19a-3p	99	−0.47
FZD3	hsa-miR-153-3p	97	−0.32

Table 2 (continued)

Genes	Predicted miRNAs	Context++ score percentile	Weighted context++ score
DAAM1	hsa-miR-6077	99	−0.50
	hsa-miR-29b-1-5p	99	−0.66
	hsa-miR-29b-3p	99	−0.60
	hsa-miR-29a-3p	99	−0.60
	hsa-miR-29c-3p	99	−0.60

Table 3

MicroRNAs (miRNAs) selection and co-differentially expressed genes (Co-DEGs) by miRDB.

Genes	Predicted miRNAs	Target Score
CCL20	hsa-miR-1322	95
	hsa-miR-3688-3p	94
	hsa-miR-5692a	94
CXCL1	hsa-miR-532-5p	92
	hsa-miR-570-3p	89
	hsa-miR-5584-3p	88
CXCL5	hsa-miR-95-5p	87
	hsa-miR-1277-5p	100
	hsa-miR-5011-5p	100
	hsa-miR-5692c	99
	hsa-miR-4776-3p	99
CXCL8	hsa-miR-5692b	99
	hsa-miR-5692a	100
	hsa-miR-140-3p	94
	hsa-miR-3671	92
	hsa-miR-548at-5p	92
CXCR4	hsa-miR-153-5p	89
	hsa-miR-139-5p	97
	hsa-miR-548bc	96
	hsa-miR-548a-3p	96
	hsa-miR-548f-3p	96
IL13RA1	hsa-miR-548az-3p	96
	hsa-miR-3119	94
	hsa-miR-147a	92
	hsa-miR-11181-5p	96
	hsa-miR-4256	95
LIF	hsa-miR-196a-1-3p	95
	hsa-miR-29c-3p	95
	hsa-miR-29a-3p	94
	hsa-miR-29b-3p	94
	hsa-miR-3121-3p	94
TNFRSF1B	hsa-miR-495-3p	100
	hsa-miR-5688	100
	hsa-miR-4478	87
	hsa-miR-670-5p	87
	hsa-miR-7160-5p	86
TNFRSF12A	hsa-miR-4313	95
	hsa-miR-548at-5p	90
	hsa-miR-6887-3p	89
	hsa-miR-6867-5p	100
	hsa-miR-4672	92
INHBA	hsa-miR-4789-5p	92
	hsa-miR-6861-5p	88
	hsa-miR-6811-3p	87
	hsa-miR-30a-5p	100
	hsa-miR-3163	100
FZD3	hsa-miR-3662	100
	hsa-miR-30c-5p	100
	hsa-miR-1250-3p	100
	hsa-miR-153-5p	100
	hsa-miR-7110-3p	97
ZNR3	hsa-miR-6502-3p	97
	hsa-miR-1827	97
	hsa-miR-10523-5p	98
	hsa-miR-3978	97
	hsa-miR-19a-3p	96
PRICKLE2	hsa-miR-19b-3p	96
	hsa-miR-520 h	95
	hsa-miR-449b-3p	99
	hsa-miR-7976	94
	hsa-miR-4683	94
FRAT1	hsa-miR-345-3p	92
	hsa-miR-3919	90

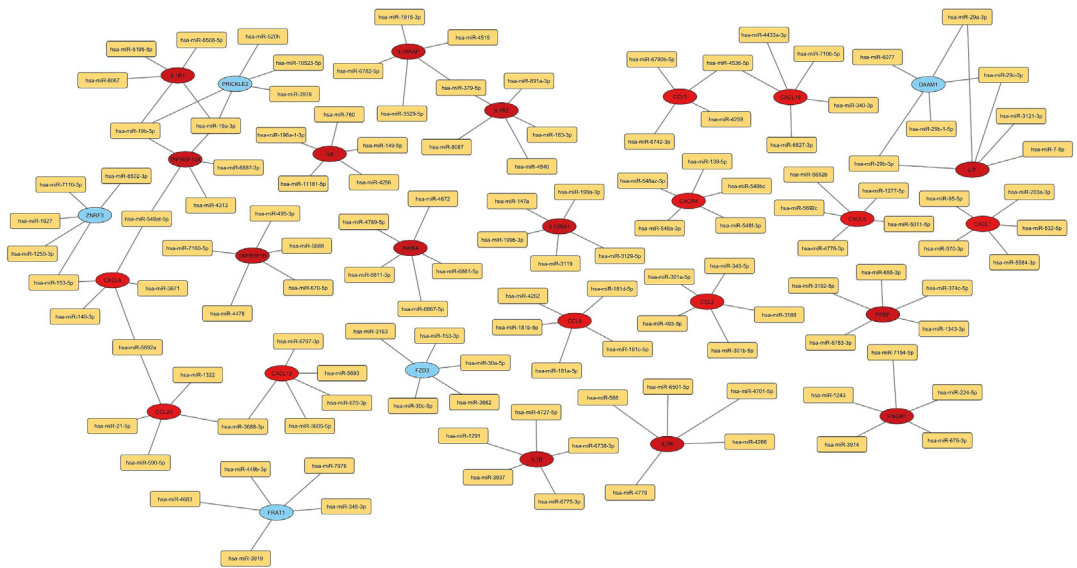


Fig. 8. MicroRNA (miRNA)-messenger RNA (mRNA) network in intracerebral hemorrhage (ICH).

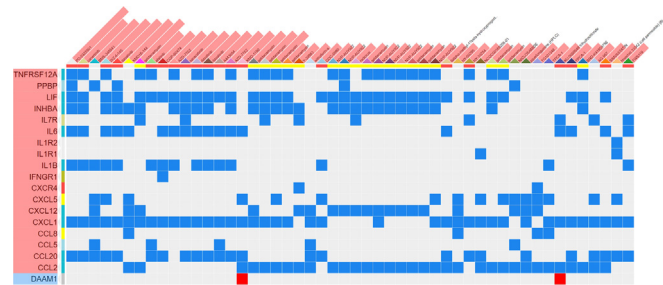


Fig. 9. Matrix of top small-molecule compounds with potential therapeutic effects on intracerebral hemorrhage (ICH). The top ranked L1000 perturbations (e.g. those with most similar or anti-similar signatures) are shown as columns with red labels that indicate their score. L1000 perturbation gene signatures are depicted as columns of the matrix with red and blue squares indicating their effect on gene expression. (For interpretation of the references to color in this figure legend, the reader is referred to the web version of this article.)

were including cytokine – cytokine receptor interaction and Wnt signaling pathway. Most of these key genes were related to inflammatory response, which was the core link of ICH injury. Studies had shown that abnormal expression of inflammation-related genes was the genetic basis of ICH, and targeted therapy for these genes may provide a new direction for the prevention and treatment of ICH.¹¹ The occurrence and development of ICH is mediated by multiple genes.

Neuroinflammation is among the many processes which are regulated by miRNA.^{40,41} With the aim of screening more robust and potential mRNAs that modulated ICH development, we performed intersection of twenty-seven regulated genes with differentially expressed miRNAs for further studies. After finishing the intersection, a total of 135 candidate miRNAs were obtained to predict their targeted mRNA. It is worth noticing that previous researches have shown that the majority of expressions of the miRNAs are consistent with our analysis. For instance, Hutchison et al., demonstrated that in the adult brain miR-181a/b expression is dynamically regulated by inflammatory stimuli and modifies the proliferation of astrocytes and their sensitivity to death in an experimental model of neuroinflammation.⁴² Overexpression of miR-181 inhibits glioblastoma cell proliferation, invasion and migration, arrested glioblastoma cell cycle in the G1 phase and induced glioblastoma cell apoptosis. miR-181 was demonstrated to decrease expression of CCL8 by directly interacting with its 3'-untranslated region.⁴³ miR-21-5p was overexpressed in response to the inflammatory cytokines in beta cell lines, and miR-21-5p inhibition could alleviate inflammation in beta cell lines.⁴⁴ In traumatic brain injury, miR-21-5p suppressed inflammation by regulating the expression of inflammatory cytokines and NF- κ B signaling and inhibited cellular apoptosis by regulating the expression of apoptosis factors and Akt signalling.⁴⁵ The results of Maranini et al., indicated that miR-21-5p play opposite but fundamental roles during SARS-CoV-2 infection.⁴⁶ MiR-21-5p directly target CCL20, whose overexpression fosters T-cell activation. Therefore,

Table 4
Potential drugs or small molecules that can reverse the expression change in identified differentially expressed genes (DEGs) through L1000CDS² data.

Candidate drugs	Cell line	Dose	Time	Overlap score	Reversible gene expressions
PD-0325901	HME1	10um	3 h	0.3478	CCL20, CXCL1, IL1B, IL6, INHBA, LIF, PPBP, and TNFRSF12A
Geldanamycin	HA1E	10um	24.0 h	0.3043	CCL2, CXCL1, CXCL12, IL7R, INHBA, LIF, and TNFRSF12A
XMD16-144	HA1E	1.11um	3 h	0.3043	CCL2, CCL8, CXCL1, CXCL12, CXCL5, IL6, and INHBA
Dasatinib	HME1	10um	3 h	0.3043	CCL20, CXCL1, IL1B, IL6, INHBA, LIF, and PPBP
WZ-4-145	HME1	10um	3 h	0.3043	CCL20, CXCL1, CXCL5, IL1B, IL6, INHBA, LIF, and TNFRSF12A
BMS-345541	HME1	3.33um	3 h	0.3043	CCL20, CCL5, CXCL1, CXCL12, CXCL5, IL1B, and PPBP
Canertinib	HME1	10um	3 h	0.3043	CCL20, CXCL1, IL1B, IL6, INHBA, LIF, and TNFRSF12A
XMD-1150	HCC515	10um	24.0 h	0.2609	CCL2, CCL20, CXCL1, CXCL5, and IL6
AZD-7762	HME1	3.33um	3 h	0.2609	CCL20, CXCL1, IL1B, IL6, INHBA, LIF, and TNFRSF12A
A443654	HME1	1.11um	3 h	0.2609	CCL20, CCL5, CXCL1, IL1B, IL6, and LIF
Saracatinib	HME1	10um	3 h	0.2609	CCL20, CXCL1, IL6, IL7R, INHBA, and LIF
CGP-60474	HME1	10um	3 h	0.2609	CCL20, CXCL1, IFNGR1, IL1B, IL6, and LIF
Afatinib	HME1	0.12um	3 h	0.2609	CCL20, CCL5, CXCL1, IL1B, LIF, and TNFRSF12A

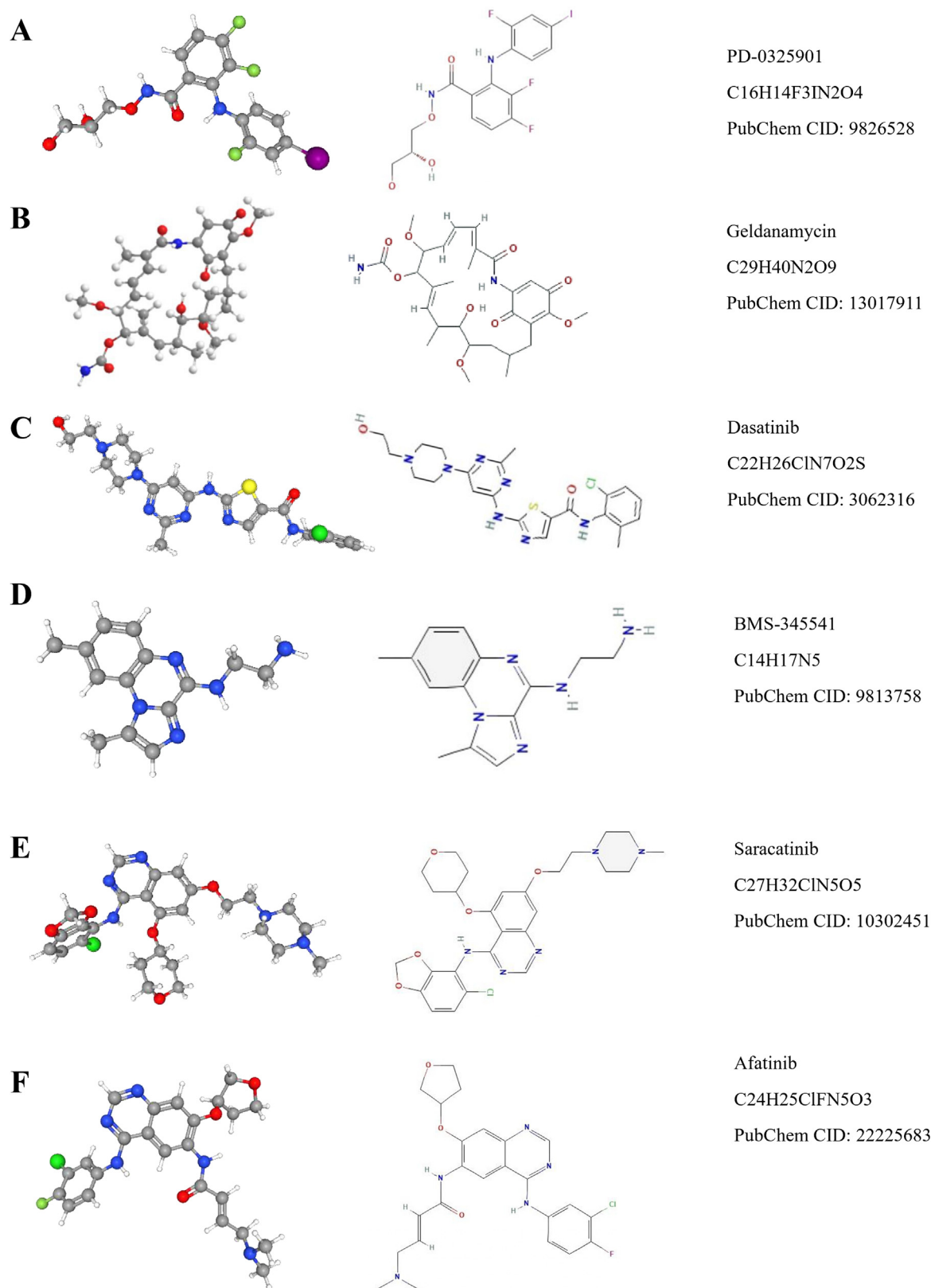


Fig. 10. 3D and 2D structures of potential 6 anti-inflammatory and neuroprotective drugs against 19 differentially expressed genes (DEGs) were analyzed using the L1000CDS2 database in intracerebral hemorrhage (ICH). (A) The chemical molecular structures of PD-0325901, (B) Geldanamycin, (C) Dasatinib, (D) BMS-345541, (E) Saracatinib, and (F) Afatinib.

the strong correlation between this miR-21-5p and CCL20 and disease severity indicates that this miRNA might be key regulators of COVID-19 pathogenesis and host immune response. Nevertheless,

the validation of these miRNA-mRNA pairs is required for elucidating their precise mechanism underlying development neuroinflammation after ICH.

Table 5
Repositioned drug candidates in intracerebral hemorrhage (ICH).

Drug	Indication	Mechanism of action	References
PD-0325901	Anti-inflammatory effect. Enhanced vascularization	ERK inhibitor	16–18
Geldanamycin	Protect mature astrocytes from necrotic cell death and young astrocytes from apoptotic death. Reduce ICH-induced brain edema and neurological deficits. Neuroprotective effect and protects brain tissue from focal ischemia	Inhibitor of hsp90	19–25
Dasatinib	Anti-inflammatory effect and can reduced microglial activation. Has immunomodulating properties and can cross the blood–brain barrier	Tyrosine kinase inhibitor	26–28
BMS-345541	Anti-inflammatory effect. Neuroprotective effect and protects brain tissue from focal ischemia	IKK inhibitor	29
Saracatinib	Anti-inflammatory effect. Modulates neuroinflammation	Tyrosine kinase inhibitor	29,30
Afatinib	Anti-inflammatory effect. Inhibits neuroinflammation and can cross the blood–brain barrier	Inhibitor of EGFR tyrosine kinases	31–34

L1000CDS² is a database that covers the interactions among diseases, gene expression patterns, and small-molecule compounds. It is often used to screen for small-molecule compounds with therapeutic effects on some diseases.⁴⁷ Using L1000CDS² analysis, we identified six small molecule drugs, one of which was geldanamycin; geldanamycin previously strong reported to have a salutary effect in cases of ICH and ischemic stroke (IS). Geldanamycin is commonly used as the prototype of a class of antitumor drugs targeting the heat shock protein 90 family of molecular chaperones and has been shown to have significant anti-inflammatory effects.⁴⁸ A recent study demonstrated that geldanamycin post-treatment is neuroprotective in the mouse model of ICH.⁴⁹ Geldanamycin administration results in reduction of inflammation, preservation of blood–brain-barrier and amelioration of neurobehavioral deficits after an insult possibly by upregulation of heat shock protein 72. The geldanamycin readily crosses the blood–brain barrier (BBB) and is a promising option for the treatment of clinical stroke.²⁵ Geldanamycin treatment induces HSPs and blocks the activation of p44/42 MAPK in experimental stroke, which may in part account for the resulting neuroprotection. Although the dasatinib, BMS-345541, saracatinib, and afatinib have been reported to be associated with the treatment of ICH, the mechanisms underlying their therapeutic actions still require further research. In addition, we found that PD-0325901 has an anti-inflammatory effect that may contribute to the treatment of ICH.

Gene regulatory network plays an important role in the pathophysiological process of ICH. The results of this study provide a new and important concept for the development of therapeutic targets/biomarkers specific for ICH, understanding the mechanisms of secondary damage and personalized medicine. However, it is important to recognize that this study is based on *in silico* analysis, and although the results are theoretically sound, they have not yet been confirmed experimentally. Although the use of an external validation dataset in the present study may serve to some extent as a viable alternative to experimental validation,

we hypothesize that experimental investigation and *in vitro* and *in vivo* validation would be a more robust approach.

5. Conclusions

Taken above, our bioinformatics analysis identified 325 upregulated and 103 downregulated DEGs of ICH. The top 27 genes may be involved in the pathological process as neuroinflammation of ICH and ultimately affect their prognosis through cytokine – cytokine receptor interaction and Wnt signaling pathway. At the same time, we constructed a miRNA–mRNA network which may play crucial roles in the pathogenesis of ICH. In addition, this study identified small-molecule compounds that may be efficacious in the treatment of secondary brain injury induced by ICH. This study may offer a novel idea for the treatment of ICH; however, further clinical studies are still needed to validate these findings.

ARRIVE guidelines statement

The authors have read the ARRIVE guidelines, and the manuscript was prepared and revised according to the ARRIVE guidelines.

Ethical Statement

This study utilized publicly available datasets from GEO. All data were anonymized and obtained in accordance with the ethical standards of the original studies. Ethical approval and informed consent for the original data generation were addressed by the respective contributing institutions, as referenced in the original publications. No additional ethical approval was required for this secondary analysis.

Funding

This work was supported by the Bashkir State Medical University Strategic Academic Leadership Program (PRIORITY-2030).

CRediT authorship contribution statement

Ilgiz Gareev: Writing – review & editing, Writing – original draft, Project administration. **Ozal Beylerli:** Validation, Data curation, Conceptualization. **Elmar Musaev:** Visualization, Methodology, Investigation. **Chunlei Wang:** Software, Data curation, Conceptualization. **Valentin Pavlov:** Supervision, Methodology, Investigation.

Data availability

All relevant raw data are freely available to any researchers who wish to use them for non-commercial purposes while preserving any necessary confidentiality and anonymity. The datasets are available on request to the corresponding author.

Declaration of Competing Interest

The authors declare that they have no known competing financial interests or personal relationships that could have appeared to influence the work reported in this paper. All the authors have consented to the publication of this manuscript.

References

- Pavlov V, Beylerli O, Gareev I, Torres Solis LF, Solís Herrera A, Aliev G. COVID-19-Related Intracerebral Hemorrhage. *Front Aging Neurosci.* 2020 Oct;22(12). <https://doi.org/10.3389/fnagi.2020.600172>. 600172.

2. Sansing LH. Intracerebral Hemorrhage. *Semin Neurol*. 2016 Jun;36(3):223–224. <https://doi.org/10.1055/s-0036-1583296>.
3. Zhu H, Wang Z, Yu J, et al. Role and mechanisms of cytokines in the secondary brain injury after intracerebral hemorrhage. *Prog Neurobiol*. 2019 Jul;178. <https://doi.org/10.1016/j.pneurobio.2019.03.003> 101610.
4. Alsbrook DL, Di Napoli M, Bhatia K, et al. Neuroinflammation in Acute Ischemic and Hemorrhagic Stroke. *Curr Neurol Neurosci Rep*. 2023 Aug;23(8):407–431. <https://doi.org/10.1007/s11910-023-01282-2>.
5. Gareev I, Beylerli O, Tamrazov R, et al. Methods of miRNA delivery and possibilities of their application in neuro-oncology. *Noncoding RNA Res.* 2023 Oct 7;8(4):661–674. <https://doi.org/10.1016/j.ncrna.2023.10.002>.
6. Li L, Wang P, Zhao H, Luo Y. Noncoding RNAs and Intracerebral Hemorrhage. *CNS Neurol Disord Drug Targets*. 2019;18(3):205–211. <https://doi.org/10.2174/1871527318666190204102604>.
7. Gareev I, Beylerli O, Liang Y, et al. The Role of Mitochondria-Targeting miRNAs in Intracerebral Hemorrhage. *Curr Neuropharmacol*. 2023;21(5):1065–1080. <https://doi.org/10.2174/1570159X2066620507021445>.
8. Xu D, Gareev I, Beylerli O, Pavlov V, Le H, Shi H. Integrative bioinformatics analysis of miRNA and mRNA expression profiles and identification of associated miRNA-mRNA network in intracranial aneurysms. *Noncoding RNA Res.* 2024 Jan 9;9(2):471–485. <https://doi.org/10.1016/j.ncrna.2024.01.004>.
9. Zou R, Zhang D, Lv L, et al. Bioinformatic gene analysis for potential biomarkers and therapeutic targets of atrial fibrillation-related stroke. *J Transl Med*. 2019 Feb 13;17(1):45. <https://doi.org/10.1186/s12967-019-1790-x>.
10. Rosell A, Vilalta A, García-Bercozo T, et al. Brain perihematoma genomic profile following spontaneous human intracerebral hemorrhage. *PLoS One*. 2011 Feb 2;6(2):e16750.
11. Liu Z, Zhang R, Chen X, et al. Identification of hub genes and small-molecule compounds related to intracerebral hemorrhage with bioinformatics analysis. *PeerJ*. 2019 Oct;25(7):e7782.
12. Zhang K, Liu C, Hu C, Lin P, Qi Q, Jia H, Tang J, Yu X. Long non-coding RNA AC245100.4 activates the PI3K/AKT pathway to promote Pca cell proliferation by elevating PAR2. *Heliyon*. 2023 Jun 3;9(6):e16870. doi: 10.1016/j.heliyon.2023.e16870.
13. Shi L, Wen Z, Li H, Song Y. Identification of Hub Genes Associated With Tuberculous Pleurisy by Integrated Bioinformatics Analysis. *Front Genet*. 2021 Dec;3(12). <https://doi.org/10.3389/fgene.2021.730491> 730491.
14. Agarwal V, Bell GW, Nam JW, Bartel DP. Predicting effective microRNA target sites in mammalian mRNAs. *Elife*. 2015 Aug;12(4):e05005.
15. Witkos TM, Koscińska E, Krzyzosiak WJ. Practical Aspects of microRNA Target Prediction. *Curr Mol Med*. 2011 Mar;11(2):93–109. <https://doi.org/10.2174/156652411794859250>.
16. Avolio E, Katara R, Thomas AC, et al. Cardiac pericyte reprogramming by MEK inhibition promotes arteriogenesis and angiogenesis of the ischemic heart. *J Clin Invest*. 2022 May 16;132(10):e152308.
17. De M, Serpa G, Zuiker E, et al. MEK1/2 inhibition decreases pro-inflammatory responses in macrophages from people with cystic fibrosis and mitigates severity of illness in experimental murine methicillin-resistant *Staphylococcus aureus* infection. *Front Cell Infect Microbiol*. 2024 Jan;30(14):1275940. <https://doi.org/10.3389/fcimb.2024.1275940>.
18. Jiang T, Gong Y, Zhang W, et al. PD0325901, an ERK inhibitor, attenuates RANKL-induced osteoclast formation and mitigates cartilage inflammation by inhibiting the NF- κ B and MAPK pathways. *Bioorg Chem*. 2023 Mar;132. <https://doi.org/10.1016/j.bioorg.2022.106321> 106321.
19. Xu L, Ouyang YB, Giffard RG. Geldanamycin reduces necrotic and apoptotic injury due to oxygen-glucose deprivation in astrocytes. *Neural Res*. 2003 Oct;25(7):697–700. <https://doi.org/10.1179/016164103101202183>.
20. Manaenko A, Fathali N, Williams S, Lekic T, Zhang JH, Tang J. Geldanamycin reduced brain injury in mouse model of intracerebral hemorrhage. *Acta Neurochir Suppl*. 2011;111:161–165. https://doi.org/10.1007/978-3-7091-0693-8_27.
21. Wen XR, Li C, Zong YY, et al. Dual inhibitory roles of geldanamycin on the c-Jun NH2-terminal kinase 3 signal pathway through suppressing the expression of mixed-lineage kinase 3 and attenuating the activation of apoptosis signal-regulating kinase 1 via facilitating the activation of Akt in ischemic brain injury. *Neuroscience*. 2008 Oct 15;156(3):483–497. <https://doi.org/10.1016/j.neuroscience.2008.08.006>.
22. Lu A, Ran R, Parmentier-Batteur S, Nee A, Sharp FR. Geldanamycin induces heat shock proteins in brain and protects against focal cerebral ischemia. *J Neurochem*. 2002 Apr;81(2):355–364. <https://doi.org/10.1046/j.1471-4159.2002.00835.x>.
23. Yin XH, Han YL, Zhuang Y, Yan JZ, Li C. Geldanamycin inhibits Fas signaling pathway and protects neurons against ischemia. *Neurosci Res*. 2017 Nov;124:33–39. <https://doi.org/10.1016/j.neures.2017.05.003>.
24. Kwon HM, Kim Y, Yang SI, Kim YJ, Lee SH, Yoon BW. Geldanamycin protects rat brain through overexpression of HSP70 and reducing brain edema after cerebral focal ischemia. *Neural Res*. 2008 Sep;30(7):740–745. <https://doi.org/10.1179/174313208X289615>.
25. Karabiyikoglu M, Hua Y, Keep RF, Xi G. Geldanamycin treatment during cerebral ischemia/reperfusion attenuates p44/42 mitogen-activated protein kinase activation and tissue damage. *Acta Neurochir Suppl*. 2013;118:39–43. https://doi.org/10.1007/978-3-7091-1434-6_6.
26. Futosi K, Németh T, Pick R, Vántus T, Walzog B, Mócsai A. Dasatinib inhibits proinflammatory functions of mature human neutrophils. *Blood*. 2012 May 24;119(21):4981–4991. <https://doi.org/10.1182/blood-2011-07-369041>.
27. Ryu KY, Lee HJ, Woo H, et al. Dasatinib regulates LPS-induced microglial and astrocytic neuroinflammatory responses by inhibiting AKT/STAT3 signaling. *J Neuroinflammation*. 2019 Oct 26;16(1):190. <https://doi.org/10.1186/s12974-019-1561-x>.
28. Dhawan G, Combs CK. Inhibition of Src kinase activity attenuates amyloid associated microgliosis in a murine model of Alzheimer's disease. *J Neuroinflammation*. 2012 Jul;2(9):117. <https://doi.org/10.1186/1742-2094-9-117>.
29. Herrmann O, Baumann B, de Lorenzi R, Muhammad S, Zhang W, Kleesiek J, Malfertheiner M, Köhrmann M, Potrovita I, Maegele I, Beyer C, Burke JR, Hasan MT, Bujard H, Wirth T, Pasparakis M, Schwaninger M. IKK mediates ischemia-induced neuronal death. *Nat Med*. 2005 Dec;11(12):1322–9. doi: 10.1038/nm1323.
30. Sharma S, Carlson S, Gregory-Flores A, Hinojo-Perez A, Olson A, Thippeswamy T. Mechanisms of disease-modifying effect of saracatinib (AZD0530), a Src/Fyn tyrosine kinase inhibitor, in the rat kainate model of temporal lobe epilepsy. *Neurobiol Dis*. 2021 Aug;156. <https://doi.org/10.1016/j.nbd.2021.105410> 105410.
31. Li J, Liu X, Liu Y, et al. Saracatinib inhibits necroptosis and ameliorates psoriatic inflammation by targeting MLKL. *Cell Death Dis*. 2024 Feb 8;15(2):122. <https://doi.org/10.1038/s41419-024-06514-y>.
32. Chen YJ, Hsu CC, Shiao YJ, Wang HT, Lo YL, Lin AMY. Anti-inflammatory effect of afatinib (an EGFR-TKI) on OGD-induced neuroinflammation. *Sci Rep*. 2019 Feb 21;9(1):2516. <https://doi.org/10.1038/s41598-019-38676-7>.
33. Xie S, Liang J, Zhao Y, et al. The second-generation tyrosine kinase inhibitor afatinib inhibits IL-1 β secretion via blocking assembly of NLRP3 inflammasome independent of epidermal growth factor receptor signaling in macrophage. *Mol Immunol*. 2023 Jan;153:135–145. <https://doi.org/10.1016/j.molimm.2022.11.009>.
34. Linnerbauer M, Löfflein L, Vandrey O, et al. Intranasal delivery of a small-molecule ErbB inhibitor promotes recovery from acute and late-stage CNS inflammation. *JCI Insight*. 2022 Apr 8;7(7):e154824.
35. Chen Y, Chen S, Chang J, Wei J, Feng M, Wang R. Perihematomal Edema After Intracerebral Hemorrhage: An Update on Pathogenesis, Risk Factors, and Therapeutic Advances. *Front Immunol*. 2021 Oct;19(12). <https://doi.org/10.3389/fimmu.2021.740632> 740632.
36. Tobieson L, Gard A, Ruscher K, Marklund N. Intracerebral Proinflammatory Cytokine Increase in Surgically Evacuated Intracerebral Hemorrhage: A Microdialysis Study. *Neurocrit Care*. 2022 Jun;36(3):876–887. <https://doi.org/10.1007/s12028-021-01389-9>.
37. Yao Y, Tsirka SE. Chemokines and their receptors in intracerebral hemorrhage. *Transl Stroke Res*. 2012 Jul;3(Suppl 1):70–79. <https://doi.org/10.1007/s12975-012-0155-z>.
38. Jridi I, Canté-Barrett K, Pike-Overzet K, Staal FJT. Inflammation and Wnt Signaling: Target for Immunomodulatory Therapy? *Front Cell Dev Biol*. 2021 Feb;4(8). <https://doi.org/10.3389/fcell.2020.615131> 615131.
39. Zhou Y, Jin J, Feng M, Zhu D. Wnt Signaling in Inflammation in Tissue Repair and Regeneration. *Curr Protein Pept Sci*. 2019;20(8):829–843. <https://doi.org/10.2174/1389203720666190507094441>.
40. Gareev I, de Jesus Encarnacion Ramirez M, Goncharov E, Ivliev D, Shumadalova A, Ilyasova T, Wang C. MiRNAs and lncRNAs in the regulation of innate immune signaling. *Noncoding RNA Res*. 2023 Aug 1;8(4):534–541. doi: 10.1016/j.ncrna.2023.07.002.
41. Gareev I, Beylerli O, Yang G, et al. The current state of MiRNAs as biomarkers and therapeutic tools. *Clin Exp Med*. 2020 Aug;20(3):349–359. <https://doi.org/10.1007/s10238-020-00627-2>.
42. Hutchison ER, Kawamoto EM, Taub DD, et al. Evidence for miR-181 involvement in neuroinflammatory responses of astrocytes. *Glia*. 2013 Jul;61(7):1018–1028. <https://doi.org/10.1002/glia.22483>.
43. Zhai F, Chen X, He Q, et al. MicroRNA-181 inhibits glioblastoma cell growth by directly targeting CCL8. *Oncol Lett*. 2019 Aug;18(2):1922–1930. <https://doi.org/10.3892/ol.2019.10480>.
44. Lakhter AJ, Pratt RE, Moore RE, et al. Beta cell extracellular vesicle miR-21-5p cargo is increased in response to inflammatory cytokines and serves as a biomarker of type 1 diabetes. *Diabetologia*. 2018;61:1124–1134. <https://doi.org/10.1007/s00125-018-4559-5>.
45. Ge XT, Huang S, Gao H, et al. miR-21-5p alleviates leakage of injured brain microvascular endothelial barrier in vitro through suppressing inflammation and apoptosis. *Brain Res*. 2016;1650:31–40. <https://doi.org/10.1016/j.brainres.2016.07.015>.
46. Maranini B, Ciancio G, Ferracin M, et al. microRNAs and Inflammatory Immune Response in SARS-CoV-2 Infection: A Narrative Review. *Life (basel)*. 2022 Feb 15;12(2):288. <https://doi.org/10.3390/life12020288>.
47. Chen S, Lv J, Luo Y, Chen H, Ma S, Zhang L. Bioinformatic Analysis of Key Regulatory Genes in Adult Asthma and Prediction of Potential Drug Candidates. *Molecules*. 2023 May 15;28(10):4100. <https://doi.org/10.3390/molecules28104100>.
48. Fukuyo Y, Hunt CR, Horikoshi N. Geldanamycin and its anti-cancer activities. *Cancer Lett*. 2010 Apr 1;290(1):24–35. <https://doi.org/10.1016/j.canlet.2009.07.010>.
49. Manaenko A, Fathali N, Chen H, et al. Heat shock protein 70 upregulation by geldanamycin reduces brain injury in a mouse model of intracerebral hemorrhage. *Neurochem Int*. 2010 Dec;57(7):844–850. <https://doi.org/10.1016/j.neuint.2010.09.001>.